JMEPEG (2017) 26:4040–4045
DOI: 10.1007/s11665-017-2827-z

1059-9495/$19.00

Cooling Curve Analysis of Micro- and Nanographite Particle-Embedded Salt-PCMs for Thermal Energy Storage Applications

R. Sudheer and K.N. Prabhu

(Submitted January 20, 2017; in revised form May 7, 2017; published online July 24, 2017)

In recent years, the focus of phase change materials (PCM) research was on the development of salt mixtures with particle additives to improve their thermal energy storage (TES) functionalities. The effect of addition of microsized (50 µm) and nanosized (400 nm) graphite particles on TES parameters of potassium nitrate was analyzed in this work. A novel technique of computer-aided cooling curve analysis was employed here to study the suitability of large inhomogeneous PCM samples. The addition of graphite micro- and nanoparticles reduced the solidification time of the PCM significantly enhancing the heat removal rates, in the first thermal cycle. The benefits of dispersing nanoparticles diminished in successive 10 thermal cycles, and its performance was comparable to the microparticle-embedded PCM thereafter. The decay of TES functionalities on thermal cycling is attributed to the agglomeration of nanoparticles which was observed in SEM images. The thermal diffusivity property of the PCM decreased with addition of graphite particles. With no considerable change in the cooling rates and a simultaneous decrease in thermal diffusivity, it is concluded that the addition of graphite particles increased the specific heat capacity of the PCM. It is also suggested that the additive concentration should not be greater than 0.1% by weight of the PCM sample.

Keywords CACCA, graphite particles, salt-PCM, thermal energy storage

1. Introduction

The applicability of energy storage systems in designing efficient power plants has opened immense scope for the development of superior energy storage materials and energy transfer techniques. Among various energy systems, thermal energy storage (TES) systems are most the attractive. TES systems had substantial influence in sectors from chemical storage, food preservation, cooling channels, air conditioning to energy generation in solar power plants. Every application is constrained on the temperature of operation and the required energy density. The use of phase changing materials improved the TES systems offering higher energy densities compared to that accessible from the sensible heat TES systems. Salt-PCMs have been successfully used as TES materials on virtue of their high energy capacity and good chemical stability at temperatures around the melting point. They fall short of ideal characteristics of a TES material due to poor thermal conductivity and low viscosity in the molten state.

In recent years, modified PCMs were developed with additives to improve their TES parameters. Solid particles are added as they conduct heat much better than the base liquids. The major limitation of such fluids is the settlement of particles. The nanosized particles are expected to stay suspended much longer compared to microparticles due to their high surface/volume ratio which is thousand times larger than that of microparticles. A large surface area leads to enhanced heat transfer rates. Nanofluids are prepared in two methods: (i) a single step method which simultaneously makes and disperses the nanoparticles into the base fluid and (ii) a two-step method where the nanopowders are prepared and then dispersed in the base fluid. In either case, a well-mixed and uniformly dispersed nanofluid is required to successfully attain enhancements in relevant properties. Although nanoparticles are dispersed ultrasonically in the base fluid using a bath or a probe sonicator, the dispersion is poor as the nanoparticles remain agglomerated in the two-step method (Ref 1).

Various parameters such as nanoparticle concentration, size and temperature had significant influence on the thermal conductivity of the nanofluids. Experimental results show that thermal conductivity of a nanofluid is nonlinearly related to the concentration of the nanoparticle addition into the base fluid (Ref 2). Das et al. (Ref 3) reported a strong temperature-dependent thermal conductivity in nanofluids. This dependence was due to the Brownian motion of nanoparticles.

Most of the research on nanofluids was performed with water or other organic liquids as the base fluids. With molten salts, the response to nanoparticle addition is expected to differ from the other. On considering salts as phase changing materials for energy storage purposes, many parameters other than thermal conductivity are considered to study their suitability

Nanoparticle-embedded nanosalts have been reported to show an increase in specific heat capacity. Cheiruzzi et al. (Ref 4) prepared nanosalts of sodium nitrate and potassium nitrate eutectic, often known as the solar salt, with nanoparticles of SiO_2, Al_2O_3, TiO_2 and SiO_2-Al_2O_3 mixture. They observed an increase in specific heat capacity along with a drop in the melting point of the PCM at all concentrations of nanopar-

R. Sudheer and **K.N. Prabhu**, Department of Metallurgical and Materials Engineering, National Institute of Technology Karnataka, Surathkal, Karnataka 575025, India. Contact e-mail: prabhukn_2002@yahoo.co.in.

ticles. The addition of mixture of SiO_2-Al_2O_3 nanoparticles showed an increase in specific heat capacity by 57% in solid phase and 22% in liquid phase with an optimum concentration of 1% by weight of the PCM sample. Cabedo et al. (Ref 5) investigated the effect of SiO_2 nanoparticles on properties of salt-PCMs. A 25% increase in the specific heat capacity of the PCM when loaded with nanoparticles constituting 1% by weight of the sample was reported. Thermal stability of the nanosalt was also studied over 8 successive thermal cycles. Here a theoretical model based on the formation of nanolayers was assumed to explain the increase in the specific heat capacity in nanosalts. Salt ions order itself around the nanoparticles forming fractal like structures (Ref 5).

Another approach in modifying a salt-PCM is to prepare a composite of a supporting material and nanoparticles along with the phase changing salt. Here the ceramic support material is expected to improve the structural and shape stability of the PCM on melting, while the nanoparticles improve the thermophysical properties. Ge et al. (Ref 6) prepared a nanocomposite of lithium-sodium carbonate eutectic salt with MgO (ceramic support material). Graphite flakes and CNT nanoparticles were dispersed separately. Green pellets of these composites were prepared by uniaxial compression and were sintered at 550 °C. The samples were experimented over 28 thermal cycles and had no significant change in mass, transition temperatures and heat of fusion promising good thermal and chemical stability. The thermal conductivity of the PCM composite increased to 5 and 4.3 W/mK for a carbon loading of 20 and 10% by weight, respectively. On the same lines, Ye et al. (Ref 7) studied the effect of MWCNT additions to sodium carbonate salt with MgO support material. Thermal conductivity of the nanocomposite was observed to increase from 0.75 to 1.127 W/mK for MWCNT composition of 0.5%. They observed an increase in thermal conductivity of the nanocomposite with temperature, where they recorded 1.489 W/mK at 120 °C for a carbon loading of 0.5%. This enhancement in thermal conductivity was attributed to the convective heat transfer of the porous support material and the radiation heat transfer in the associated pores.

Characterization of TES materials has been carried out mostly using DSC technique. The major limitation of this technique is the small size of the test sample, in the order of milligrams. The information obtained from an inhomogeneous TES material, such as composites, of such small size would represent the property of the particular sample alone than that of the material. Heating/cooling rates of the sample too have an influence on the information obtained. The overestimation of subcooling and inaccurate prediction of phase transition temperatures are the other limitations of DSC technique. T-History method introduced by Yinping et al. (Ref 8) is another technique suitable for TES material characterization. Unlike DSC, a large sample is analyzed here along with a standard reference medium of known properties. Judicious selection of a standard reference material for high-temperature studies and selection of container material and its dimensions limit this method. The merits and demerits of both these methods were extensively discussed by Mehling and Cabeza (Ref 9), Sudheer and Prabhu (Ref 10).

In this work, the relative effect of both nano- and microsized graphite particles with varying concentrations on TES parameters of potassium nitrate was investigated. Graphite particles were chosen for being chemically stable at the operating temperatures of nitrate salts and for having density near to that of the nitrate salts offering minimum settling of particles. The nitrate salts have been successfully employed in the TES systems of concentrated solar power (CSP) plants in recent years. The temperature history of PCMs was recorded by employing computer-aided cooling curve analysis, and the other TES parameters were computed by using the Fourier technique. Further, the response of graphite additives to successive thermal cycles of the PCMs was analyzed here. Ten successive experiments of melting and freezing of the particle-embedded salt-PCMs were performed. In addition to this, the effect of high-energy ball milling method of particle dispersion on the TES parameters of PCMs was compared with that of the hand-mixing method.

2. Experimental

Fourier technique of CACCA was performed with a sample size of 1 kg in a cylindrical SS304 mold. The mold was chosen with a length/diameter ratio of 5 to ensure radial solidification of the PCM. Calibrated K-type Inconel sheath temperature sensors were used along with a thermal data acquisition system (NI USB 9213) in the experiments. Figure 1 shows the schematic sketch of the experimental setup for Fourier method. The PCM of KNO_3 was mixed with graphite particles of size 50 μm (CDH, Delhi) and 400 nm (SRL) separately to study their respective effects on the TES parameters. The PCM mass was fixed at 1 kg for every trial into which the particle additives weighing 0.1% and 0.5% of the PCM weight were added. Graphite nanoparticles were dispersed into the pulverized salt-PCM by (1) thorough hand-mixing and (2) using planetary ball milling. A high-energy planetary ball milling facility (Retch PM100, at 150 rpm, for 20 min, 87 steel balls of 10 mm diameter) was used for this purpose. Every sample was melted and then solidified for 10 cycles to analyze the thermal cycling effects on these inhomogeneous PCMs. JEOL Analytical SEM (JSM 6380LA) was used for microstructure examination of PCMs.

Computer-aided cooling curve analysis (CACCA) was employed here to record thermal history of TES materials as it has an advantage over the conventional DSC and T-history

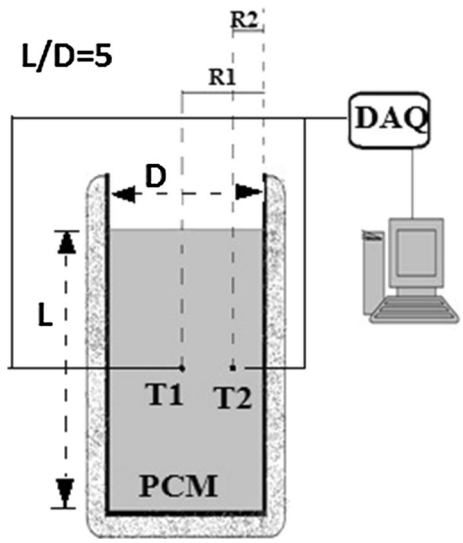

Fig. 1 Schematic sketch of the experimental setup for Fourier technique

techniques for being simple, less expensive and consistent with results. The data on phase transition temperatures, latent heat of fusion, solidification time, cooling rates, thermal diffusivity as a function of temperature, etc. can be computed by using either the Newtonian technique or the Fourier technique. The thermal gradients developed during solidification are neglected in Newtonian method, while it is incorporated in the Fourier method. Fourier technique was employed here due to low thermal conductivity of salt-PCMs which causes significant thermal gradients in the sample during solidification. Figure 1 shows the schematic sketch of the experimental setup for Fourier technique. A cylindrical mold with a length-to-diameter ratio of 5 is used for solidification of PCMs. L/D > 4 is required to attain radial solidification in cylindrical samples. Radial solidification of PCMs is mandatory in Fourier method.

The theory of Fourier technique was first suggested by Fras et al. (Ref 11). The Fourier equation with heat source can be expressed as shown in Eq 1, which can be rewritten as Eq 2 where BL_F stands for Fourier baseline. A baseline represents an imaginary line connecting the liquidus and the solidus points in the cooling curve of the sample with an assumption of no latent heat being released on solidification. The difference in the integral area of the cooling rate curve and that of its corresponding baseline (BL_F) would represent the latent heat of solidification when multiplied with the specific heat capacity of the PCM, as shown in Eq 6. During transient heat conduction, the temperature within a cylindrical sample depends on axial coordinates (z, r and θ) and time t. With an L/D ratio of 4 or more, the heat transfer takes place only in the radial direction (r axis). This ensures that the process is axially symmetric, and temperature is independent of θ coordinate. Heat conduction equation under transient conditions without any heat source in a cylindrical sample with an L/D ratio of 5 can be expressed as shown in Eq 3. Fourier technique assumes the temperature distribution at an instant of time in such a sample to be parabolic, which can be expressed as $T = Ar^2 + B$, where r is the radius of the sample. This assumption can be used to compute Eq 4. With temperature data obtained from thermocouples positioned at radii R_1 and R_2, the thermal diffusivity can be obtained from Eq 5. The CACCA technique and its mathematical equations have been discussed by Sudheer and Prabhu (Ref 10) and Djurdjevic et al. (Ref 12) in detail.

$$\frac{\partial T}{\partial t} = \alpha \nabla^2 T + \frac{1}{C_V}\frac{\partial Q}{\partial t} \quad \text{(Eq 1)}$$

$$\frac{\partial Q}{\partial t} = C_V\left(\frac{\partial T}{\partial t} - BL_F\right) \text{where } BL_F = \alpha \nabla^2 T \quad \text{(Eq 2)}$$

$$\nabla^2 T = \frac{1}{r}\frac{\partial}{\partial r}\left(r\frac{dT}{dr}\right) \quad \text{(Eq 3)}$$

$$\nabla^2 T = \frac{4(T_2 - T_1)}{R_2^2 - R_1^2} \quad \text{(Eq 4)}$$

$$\alpha = \frac{\frac{\partial T}{\partial t}}{\nabla^2 T} \quad \text{(Eq 5)}$$

$$L = \int_{t_s}^{t_e} \frac{\partial Q}{\partial t}(t)dt \text{ where } \frac{\partial Q}{\partial t} = C_V\left(\frac{\partial T}{\partial t} - BL_F\right) \quad \text{(Eq 6)}$$

3. Results and Discussion

The cooling curve of KNO_3 revealed that the PCM solidified at 335 °C as shown in Fig. 2. The solidification time for the PCM sample of size 1 kg was observed to be 850 ± 30 s. Particle addition did not influence the solidification temperature of the PCM as the composite PCM of KNO_3 and graphite particles (both micro- and nanoparticles) solidified at 335 °C. However, the solidification time decreased significantly on particle addition. The addition of 0.1% of graphite microparticles by weight of the PCM sample reduced the solidification time to 760 ± 10 s, indicating an increase in the heat removal rate by 11.8%. The addition of 0.5% of graphite microparticles further decreased the solidification time of the sample to 728 ± 10 s offering an 18% increase in heat removal rate. The sample maintained this over next 10 thermal cycles. The decrease in solidification time of the PCM is beneficial as the same amount of thermal energy can now be extracted at a much higher rate, improving the effectiveness of TES systems in power generation units. The percentage change in heat removal rate is calculated using Eq 7 shown below.

$$\%\Delta H = \frac{t_{\text{pure salt}} - t_{\text{nano salt}}}{t_{\text{nano salt}}} \times 100 \quad \text{(Eq 7)} \qquad \text{here, } \boldsymbol{t} = \text{ solidification time.}$$

Nanoparticles proved to be more effective in reducing the solidification time compared to the microparticles. The hand-mixed mixture of KNO_3 and graphite nanoparticles (0.1% and 0.5% by weight of PCM) decreased the solidification time from 850 ± 30 s to 600 s and 590 s, respectively, in the first thermal cycle (melting–freezing). The corresponding change in the heat release rate showed a significant increase of 41 and 44%, respectively. Unlike the previous case, the solidification time here increased later to 750 and 720 s, respectively, on successive thermal cycles, and remained consistent thereafter. Nanoparticles agglomerate on every cycle of melting-solidification leading to decay in the TES functions of the PCM. The benefits due to a decrease in the solidification time on addition of nanoparticles diminish in 4–5 thermal cycles, and performance was comparable to the microparticle-embedded salt-PCM thereafter. The

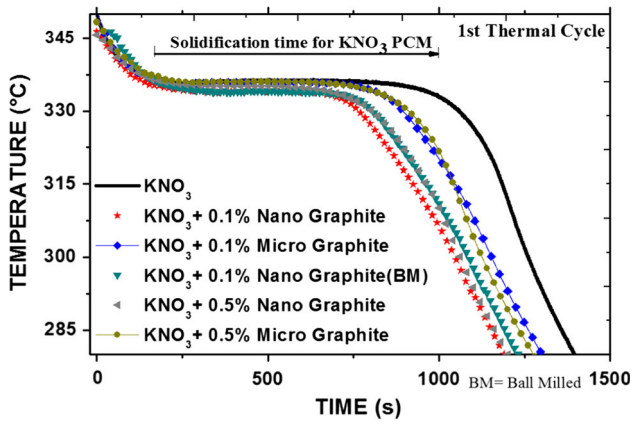

Fig. 2 Cooling curves of various PCM composites during the first thermal cycle

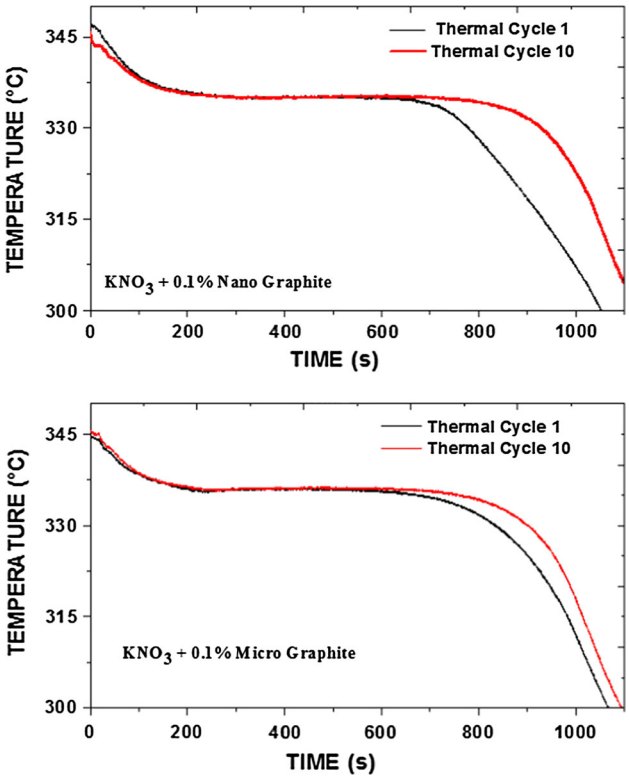

Fig. 3 Effect of thermal cycling on cooling curve of PCM composites

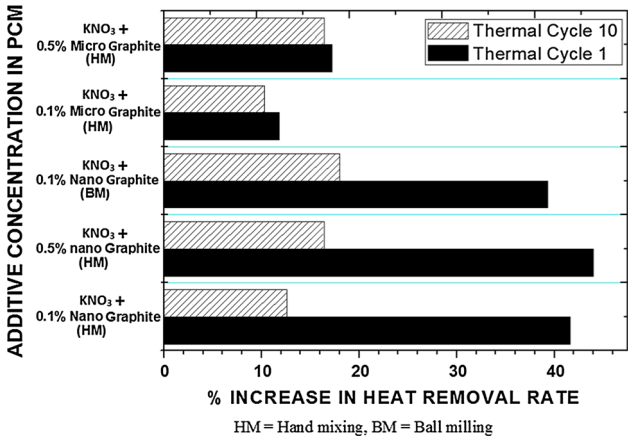

Fig. 4 Effect of thermal cycling on heat removal rate of PCMs

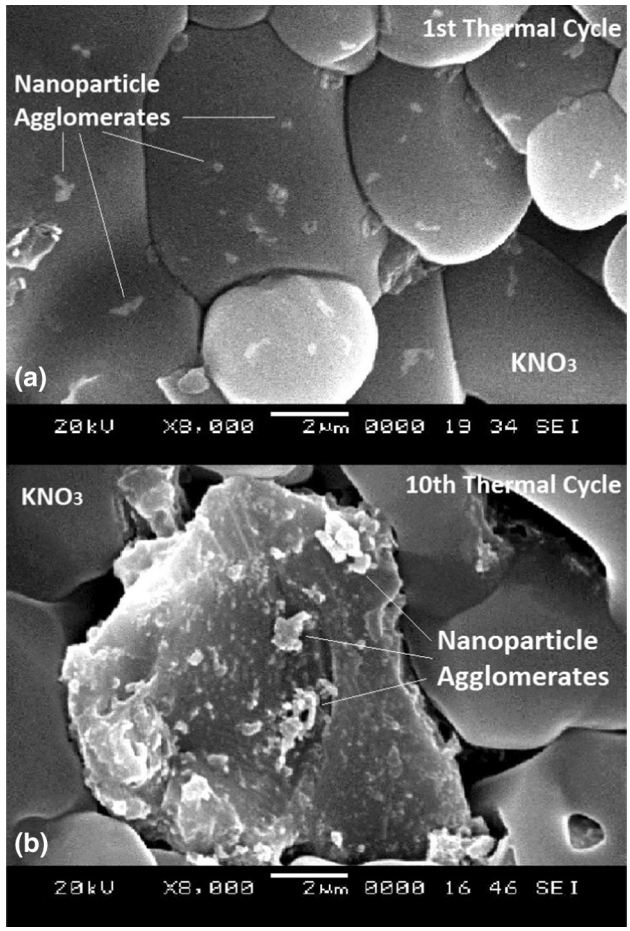

Fig. 5 SEM images of nanosalt-PCM, (a) After first thermal cycle and (b) after 10th thermal cycle

cooling curves of various PCM composites studied here are shown in Fig. 2. The cooling curves obtained from the 1st and the 10th thermal cycle of graphite particle (both nano- and micro-sized particles) added salt-PCM are shown in Fig. 3. The effect of thermal cycling of the PCM composite over the increase in heat removal rate is shown in Fig. 4.

The SEM images show significant agglomeration of graphite nanoparticles on thermal cycling. The considerable increase in solidification time over successive thermal cycling is attributed to the agglomeration of nanoparticles in the nanosalt-PCM. The SEM images of PCM composites with 0.5% of graphite nanoparticles are shown in Fig. 5.

The effect of dispersal of nanoparticles on the salt-PCM using a high-energy ball milling method was also studied as it improves homogeneity or even dispersal of nanoparticles. The PCM mixture with 0.1% graphite nanoparticle by weight solidified in 610 s in the first thermal cycle and then deteriorated to 720 ± 10 s in successive cycles. It is evident that the distribution of nanoparticles in KNO_3 sample using ball milling method had no considerable effect compared to the hand-mixing method on the solidification time. However, it is important to mention the slight improvement in the PCM's response to thermal cycling. The ball-milled sample showed relatively less decay in heat release rates over 10 successive thermal cycles compared to a hand-mixed PCM composite, which is observed in Fig. 4. The details of particle additions on PCM and its response to thermal cycles are shown in Table 1.

Another efficient tool in cooling curve analysis is the cooling rate curve. Figure 6 shows the cooling rate curve of KNO_3. It is observed that the cooling rate drops to a value close to zero during freezing of the sample and quickly increases after solidification. The nucleation and freezing transitions are not sharply observed in the cooling curve. This is reflected on the cooling rate curve as a slow transition from the solidification temperature to the point of cooling rate reversal ($\mathbf{CR_P}$). This is a point where the latent heat released during freezing of the sample is completely withdrawn from the vicinity of the thermocouple, and the sample cools thereafter over the temperature gradient. This delay is due to low thermal diffusivity of the salt-PCM. In case of PCMs of high thermal

Table 1 Effect of addition of micro-/nanoparticles on TES parameters of KNO_3 (salt-PCM)

Particle addition to PCM (by wt.%)	Thermal cycles	Solidification time (s) ± 2%	Temperature at CR_p (°C) ± 1 °C	Cooling rate at CR_p (°C/s) ± 0.01	Temperature drop in 1000 s post-CR_P (°C)	ΔH rate (%)
Nanoparticles						
Hand mixing						
0.1%	1	600	300	0.16	95	41.6
	10	755	315	0.22	99	12.6
0.5%	1	590	304	0.17	98	44.0
	10	730	315	0.21	102	16.4
Ball milling						
0.1%	1	610	324	0.28	116	39.3
	10	720	315	0.22	109	18.0
Microparticles						
Hand mixing						
0.1%	1	760	303	0.17	95	11.8
	10	770	314	0.21	100	10.3
0.5%	1	725	315	0.21	101	17.2
	10	730	314	0.23	102	16.4

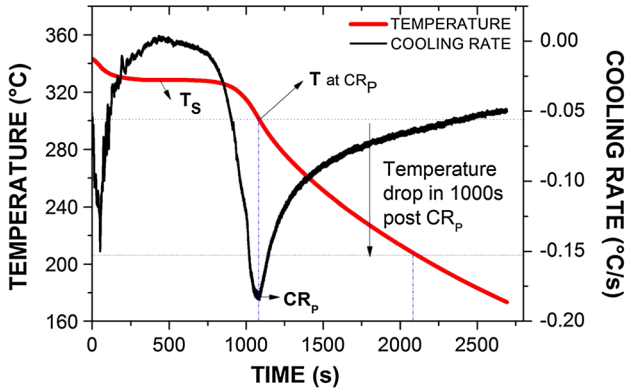

Fig. 6 Cooling curve and cooling rate curve of KNO_3 (salt-PCM)

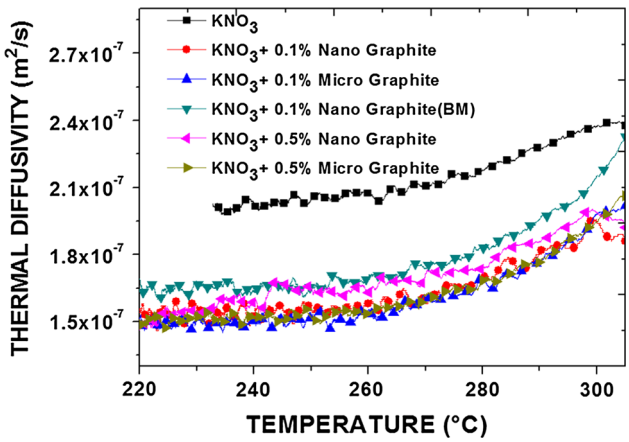

Fig. 7 Thermal diffusivity curves of various salt-PCM composites (computed using Eq 4)

diffusivity like metals, the transition will be sharp in the cooling curve and the time lag between the solidification temperature (solidus point) and the **CR_P** will be minimum.

The effect of particle addition on the cooling rate curve is shown in Table 1. It is evident that the particle additions do not have considerable influence on the cooling rates of the PCM post-solidification. All the PCM mixtures showed a drop of 98–102 °C over 1000s after CR_P except for the ball-milled sample. The ball-milled sample showed a drop of 116 °C in the first cycle which can be attributed to the uniformity in distribution of nanoparticles in the salt-PCM. This effect diminished in successive thermal cycles. The temperature at which CR_P occurred was recorded, and a peculiar trend was observed. CR_P was observed to be around 300–304 °C in all the PCM mixtures in the first thermal cycle. It increased to approximately 315 °C by the fourth cycle and remained constant thereafter. Unlike above, the ball-milled PCM mixture had CR_P at 324 °C initially which dropped to 315 °C in successive cycles.

The thermal diffusivity property of PCMs was predicted using Eq 1-4. The thermal diffusivity of the PCM post-solidification is shown in Fig. 7. The thermal diffusivity of KNO_3 decreased from 1.9–2.1 × 10^{-7} m^2/s to 1.5–1.6 × 10^{-7} m^2/s on addition of graphite particles as shown in Fig. 7. The size of the particle did not have a considerable influence on the thermal diffusivity measured. Thermal diffusivity gives an idea about how fast the heat can propagate in the PCM, and how quick a material reacts to a change in temperature. It can be represented as the ratio of thermal conductivity of a material to the product of its specific heat capacity and mass density. The absence of changes in cooling rates and a simultaneous decrease in thermal diffusivity is an indication of an increase in the specific heat capacity (SHC) of the PCM on particle addition. The increase in specific heat capacity of PCMs on addition of nanoparticles was attributed to the formation of nanolayers as discussed earlier.

One of the reasons for higher SHC of nanosalt-PCMs is the nanoparticles themselves. The SHC of a material is related to its structure. Nanoparticles have nanograined structures and expose more atoms to the surface as they possess high surface area-to-volume ratio. The surface atoms are less constrained compared to the atoms at the center. Therefore, the nanoparticles possess more energy compared to the coarse-grained particles. Wang et al. (Ref 13) recorded a blueshift in the wave number in infrared spectrum of nanograined Al_2O_3 compared to

that of coarse-grained Al_2O_3. This proves that the nanoparticles possess higher energy. Other parameters such as interfacial thermal resistance, temperature, density, thermal expansion, size effect too influence the SHC values of nanosalt-PCMs.

The anomalous increase in SHC values in molten salt is attributed to the hypothesized network of ordered layers near to the surface of nanoparticles. These networks are known as nanolayers. These semisolid layers offer higher SHC where the latent heat of fusion of the entrapped PCM is taken into consideration.

It is observed that when the additive concentration was raised by 5 times (0.1 to 0.5% by weight) the change in the heat removal rate of the PCM increased slightly by 6% and by 2% for micro- and nanoparticle-embedded salt-PCM, respectively. Further, this increase in concentration did not have any considerable effect on the cooling rate curves and thermal diffusivity curves. Highest enhancement of TES functions was obtained for a critical graphite additive concentration of 0.1% by wt of the PCM sample. It is suggested that further research on the influence of graphite particles can be directed at this additive concentration. Agglomeration of nanoparticles is the major challenge which diminishes significant enhancements observed in the TES parameters of nanosalts. Various methods such as ultrasonication or use of dispersants can be explored to extend the benefits obtained on nanoparticle addition, such as increasing the operating life of the nanosalt-PCMs.

4. Conclusion

The addition of micro- and nanosized graphite particles had a considerably different influence on the TES parameters of KNO_3. The nanoparticle-embedded PCM offered significant increase in the heat removal rates by decreasing the solidification time significantly. The enhancement in the heat removal rate in nanosalt-PCM was 40% as compared to an increase of only 12% obtained with microsalt-PCMs at concentration level of 0.1% by weight. The effects observed on addition of microparticles to the salt-PCM were consistent throughout the period of 10 thermal cycles. In contrast, the enhancements obtained initially in the nanosalt-PCM diminished over successive thermal cycles, and their performance was equivalent to the micropowder-embedded salts thereafter. The decay of TES functionalities of nanosalt-PCMs on thermal cycling is due to the agglomeration of graphite nanoparticles.

Acknowledgments

This research was supported National Institute of Technology Karnataka, India. We thank our colleagues and Mr. Dinesh, Technical Staff associated with the Casting Research Centre, Department of Metallurgical & Materials Engineering, who provided insight and expertise that greatly assisted this study.

References

1. S.K. Das, S.U.S. Choi, W. Yu, and T. Pradeep, *Nanofluids: Science and Technology*, Wiley, Hoboken, 2008, p 1–33
2. S.U.S. Choi, Z.G. Zhang, W. Yu, F.E. Lockwood, and E.A. Grulke, Anomalous Thermal Conductivity Enhancement in Nano-Tube Suspensions, *Appl. Phys. Lett.*, 2001, **79**, p 2252–2254
3. S.K. Das, N. Putra, P. Theisen, and W. Roetzel, Temperature Dependence of Thermal Conductivity Enhancement for Nanofluids, *J. Heat Transf.*, 2003, **125**, p 567–574
4. M. Chieruzzi, G.F. Cerritelli, A. Miliozzi, and J.M. Kenny, Effect of Nanoparticles on Heat Capacity of Nanofluids Based on Molten Salts as PCM for Thermal Energy Storage, *Nanoscale Res. Lett.*, 2013, **8**, p 448
5. P.A. Cabedo, R. Mondragon, L. Hernandez, R.M. Cuenca, L. Cabedo, and J.E. Julia, Increment of Specific Heat Capacity of Solar Salt with SiO_2 Nanoparticles, *Nanoscale Res. Lett.*, 2014, **9**, p 582
6. Z. Gea, F. Ye, H. Cao, G. Leng, Y. Qin, and Y. Ding, Carbonate-Salt-Based Composite Materials for Medium- and High-Temperature Thermal Energy Storage, *Particulogy*, 2014, **15**, p 77–81
7. F. Ye, Z. Ge, Y. Ding, and J. Yang, Multi-walled Carbon Nanotubes Added to Na2CO_3/MgO Composites for Thermal Energy Storage, *Particulogy*, 2014, **15**, p 56–60
8. Z. Yinping, J. Yi, and J. Yi, A Simple Method, the T-History Method, of Determining the Heat of Fusion, Specific Heat and Thermal Conductivity of Phase-Change Materials, *Meas. Sci. Technol.*, 1998, **10**, p 201–205
9. H. Mehling, L.F. Cabeza, in *Heat and cold storage with PCM: an up to date introduction into basics and applications*, *Heat and Mass Transfer series* ed., Springer 2008, p. 57–102
10. R. Sudheer and K.N. Prabhu, A Computer Aided Cooling Curve Analysis Method to Study Phase Change Materials for Thermal Energy Storage Applications, *Mater. Des.*, 2016, **95**, p 198–203
11. E. Fras, W. Kapturkiewicz, A. Burbielko, and H.F. Lopez, A New concept in thermal Analysis of Castings, *AFS Trans.*, 1993, **101**, p 505–511
12. M.B. Djurdjevic, Z. Odanovic, and N. Talijan, Characterization of the Solidification Path of AlSi5Cu (1–4at%) Alloys Using Cooling Curve Analysis, *JOM*, 2011, **63**, p 51–57
13. L. Wang, Z. Tan, S. Meng, D. Liang, and G. Li, Enhancement of Molar Heat Capacity of Nanostructured Al2O3, *J. Nanoparticle Res.*, 2001, **3**, p 483–487